Article

Journal of Vibration and Control
18(5) 684–695

DOI: 10.1177/1077546311408989
jvc.sagepub.com
SAGE

Vibration control of adjacent buildings considering pile-soil-structure interaction

Lihua Zou[1], Kai Huang[1], Liyuan Wang[1], John Butterworth[2] and Xing Ma[3]

Abstract

This paper presents an investigation of the influence of pile-soil-structure interaction (PSSI) on the vibration control of adjacent buildings with pile foundations. With the initial assumption that adjacent buildings are linked by the control actuator of an ideal hydraulic servo-system, based on the Penzien model, the calculation model for adjacent structures with piled foundations considering PSSI is established. The motion and control equations of adjacent structures are then derived, and the influences of PSSI on vibration control of adjacent buildings analyzed. Finally, the influences of soil and structural parameters on structural vibration control are investigated. The results show that the PSSI has an obvious influence on the response of adjacent structures, but little obvious influence on the change in control force. However, the soil and structural parameters, such as shear-wave velocity and pile stiffness, play a significant role in the control process.

Keywords

Adjacent building, control force, pile-soil-structure interaction, vibration control

Received: 28 April 2010; accepted: 22 March 2011

1. Introduction

Buildings in a modern city are often built close to each other because of limited available land and the need to access centralized services, making them at risk of pounding each other when responding to strong ground motion (Basili and Angelis, 2007; Luco and Barros, 1998; Lu et al., 2002). To prevent mutual pounding between adjacent buildings during an earthquake, some researchers (Kobori et al., 1988; Ni et al., 2001, 2004; Zhang and Xu, 2000; Zhang et al., 2006; Zhu et al., 2001) have proposed linking adjacent structures with control devices and using them to apply active or semi-active control.

Most studies have assumed that the controlled structures are built on fixed bases (Ni et al., 2001; Zhang and Xu, 2000; Zhu et al., 2001) despite the fact that many buildings are actually constructed on soft foundation materials (Maki et al., 2006; Zhang et al., 2006). The seismic response of an engineering structure is affected by the medium on which it is founded (Zhang et al., 2006). Compared with a corresponding fixed-base system, structural response is affected in two basic ways by soil-structure interaction (SSI). Firstly, the SSI system has an increased number of degrees-of-freedom (d.f.) with correspondingly modified dynamic characteristics. Secondly, a significant part of the vibration energy of the SSI system may be dissipated either by radiation waves emanating from the vibrating foundation–structure system back into the soil, or by hysteretic material damping in the soil. The result is that SSI systems have longer natural periods of vibration than their fixed-base counterparts. Moreover, the simplification ignores the fact that a structure experiencing SSI is not subjected to the free-field ground motion. Instead, the input motion depends on the properties

[1]Department of Civil Engineering, Fuzhou University, China
[2]Department of Civil and Environmental Engineering, University of Auckland, Auckland, New Zealand
[3]School of Natural and Built Environments, University of South Australia, Adelaide, Australia

Corresponding author:
Lihua Zou, Department of Civil Engineering, Fuzhou University, Fuzhou 350108, China
Email: Zoulihua66@163.com

of the foundation soil and the dynamic characteristics of the superstructure (Maki et al., 2006; Zhang et al., 2006).

The differences between calculation model and practical structure challenge the design of a structural control system as the dynamic characteristics of a structure are the main inputs in the control algorithm no matter what control strategy is employed. The effects would be reduced or even result in a failure of control if the differences were large enough (Wang and Shang, 2006; Zou et al., 2004; Zou and Zhao, 2005).

The importance of including the influence of SSI on the effectiveness of control for single buildings has already been emphasized in the work by Wong and Luco (1991), who studied the effectiveness of active control of seismically excited structures considering soil-structure interaction. The structure, represented by a uniform shear beam, was supported by a rigid foundation embedded in a viscoelastic soil medium. An absorbing boundary at the top of the beam acted as an active control device to cancel the reflection of the propagating vibration waves induced by vertically incident shear waves at the beam base. This work concluded that the control rule used to obtain the absorbing boundary was sensitive to the rocking of the foundation resulting from the effect of kinematical and inertial interaction. In particular, the amplitude of the structural response and the control force exerted by the absorbing boundary decreased as the soil became softer. Smith et al. (1994) and Wu and Smith (1995) studied the effects of SSI on the response of a one-storey actively controlled structure supported on a rigid rectangular foundation resting on an elastic half-space. Luco and Barros (1998) presented a model for the seismic response of a one-storey structure subjected to active control in the presence of soil-structure interaction effects. Smith and Wu (1997) presented a discussion of the effects of SSI on the formulation of active structural control algorithms, and developed two approaches for incorporating SSI effects in linear optimal control theory. Wang and Shang (2006) analyzed the influence of SSI on the control performance of multiple tuned mass dampers (MTMDs). Lin et al. (2009) analyzed the effect of SSI on vibration control effectiveness of active tendon systems for an irregular building.

The pile foundation and the rigid foundation are two of the most widely used foundations of buildings. They are usually used in high-rise buildings, which are generally the main targets of active control. PSSI and SSI have been observed by many scholars over a long period of time, but only very limited research studies have been conducted to determine their influence on active control. Almost all of these studies have focused only on the control of single buildings, and very few discussed the influence of PSSI on control of adjacent buildings. However, it is more difficult to build an accurate model of adjacent buildings than that of a single building. As a result, it will produce a larger time-delay when the adjacent building is controlled.

The purpose of this paper is to investigate the influences of PSSI on vibration control of adjacent buildings with piled foundations. Calculation models taking PSSI into account are established and their motion and vibration control equations derived. The influences of soil and structural parameters on structural vibration control are studied.

2. Model and motion equation of adjacent structures with piled foundations

The structural model of the building complex and the corresponding analytical model are shown in Figure 1. Structures A and B are k_1 and J_1-story buildings with piled foundations, and they are linked by some control devices. The superstructure and the piles are simplified to a multiple-degree-of freedom system in which all of the piles are incorporated into an equivalent pile for each structure. An equivalent bending spring is applied at the location of the pile platform to replace the rotational stiffness of the pile group. The soil surrounding the piles is simplified to an equivalent spring-mass system, connected rigidly to the mass of the equivalent pile.

In the light of the above hypothesis and model, the equations of motion of the superstructure, platform rotation and substructure of structure A can be expressed as

$$M_{sA}\ddot{X}_{sA} + C_{sA}\dot{X}_{sA} + K_{sA}X_{sA} = -M_{sA}I_{A_1}\ddot{x}_g - M_{sA}H_A\ddot{\theta}_A + B_{sA}U \tag{1}$$

$$\sum_{i=1}^{n_1} m_{sAi}h_{Ai}(\ddot{x}_g + \ddot{x}_{sAi} + h_{Ai}\ddot{\theta}_A) + c_{\theta A}\dot{\theta}_A + k_{\theta A}\theta_A = 0 \tag{2}$$

$$M_{dA}\ddot{X}_{dA} + C_{dA}\dot{X}_{dA} + K_{dA}X_{dA} = -M_{pA}I_{A_2}\ddot{x}_g + M_{eA}\ddot{X}_{fA} + C_{eA}\dot{X}_{fA} + K_{eA}X_{fA} \tag{3}$$

where M_{sA}, C_{sA} and K_{sA} are respectively the $k_1 \times k_1$ mass, damping and stiffness matrices of the superstructure; $\ddot{X}_{sA}$, $\dot{X}_{sA}$ and X_{sA} are respectively the k_1-dimensional acceleration, velocity and displacement vectors of the superstructure; M_{dA}, C_{dA} and K_{dA} are respectively the $k_2 \times k_2$ mass, damping and stiffness matrices of the substructure; $\ddot{X}_{dA}$, $\dot{X}_{dA}$ and X_{dA} are respectively

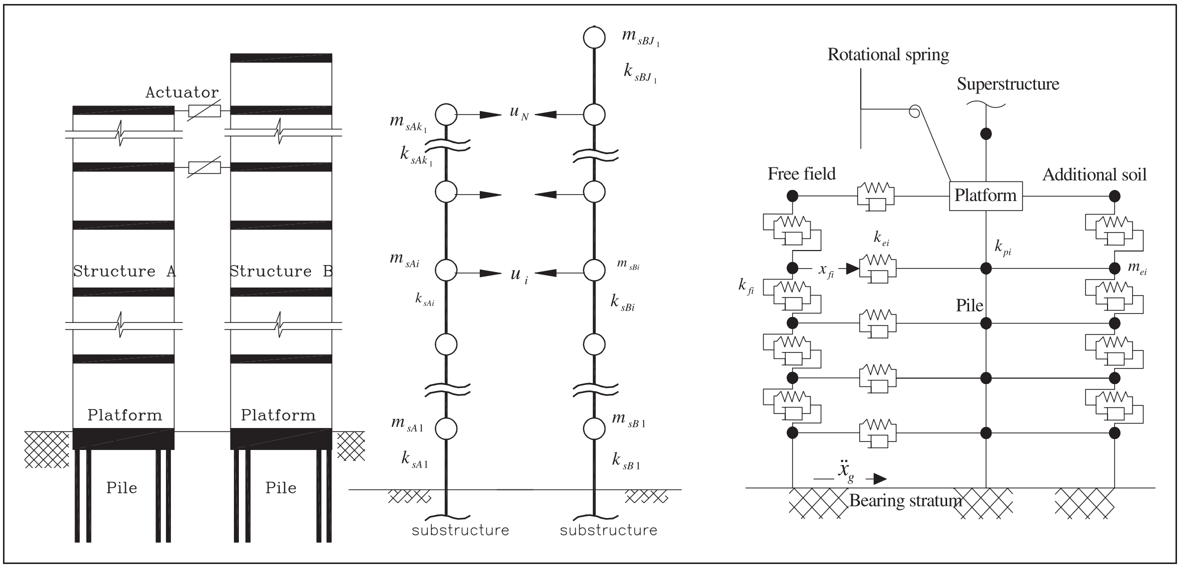

Figure 1. Calculation model of adjacent buildings. a) Sketch of structural model; b) calculation model of superstructures; c) Calculation model of substructures of adjacent buildings.

the k_2-dimensional acceleration, velocity and displacement vectors of the substructure; M_{eA}, C_{eA} and K_{eA} are respectively the $k_2 \times k_2$ mass, damping and stiffness matrices of the equivalent soil; $\ddot{X}_{fA}$, $\dot{X}_{fA}$ and X_{fA} are respectively the k_2-dimensional acceleration, velocity and displacement vectors of the unit soil column; $\ddot{x}_g$ is the ground acceleration; $c_{\theta A}$ and $k_{\theta A}$ are respectively the damping and stiffness coefficients of the platform rotation; θ_A is the rotation angle of the platform; M_{pA} is a $k_2 \times k_2$ mass matrix of the pile group; I_{A_1} and I_{A_2} are the identity vectors, H_A is a k_1-dimensional height vector of the building floors, U is the control force matrix, and B_{sA} is the location matrix of control forces. Equations (1) to (3) can be replaced by an equivalent equation

$$M_A\ddot{X}_A + C_A\dot{X}_A + K_A X_A = -M_{gA}\ddot{X}_{fgA} + B_{sA}U \qquad (4)$$

where M_A, C_A and K_A are respectively the $n_1 \times n_1$ mass, damping and stiffness matrices of system A; $\ddot{X}_A$, $\dot{X}_A$ and X_A are respectively the n_1-dimensional acceleration, velocity and displacement vectors of system A; M_{gA} is the diagonal matrix of M_A; $\ddot{X}_{fgA}$ is the acceleration vector of free field input. The matrices can be expressed as follows:

$$M_A = \begin{bmatrix} m_{sA1} & & & m_{sA1}h_{sA1} & & & \\ & \ddots & & \vdots & & & \\ & & m_{sAk_1} & m_{sAk_1}h_{sAk_1} & & & \\ m_{sA1}h_{sA1} & \cdots & m_{sAk_1}h_{sAk_1} & \sum_{i=1}^{k_1} m_{sAi}h_{sAi} & & & \\ & & & & m_{eA1}+m_{pA1} & & \\ & & & & & \ddots & \\ & & & & & & m_{eAk_2}+m_{pAk_2} \end{bmatrix}$$

$$K_A = \begin{bmatrix} k_{sA1}+k_{sA2} & -k_{sA2} & & & -k_{sA1} & & \\ -k_{sA2} & \ddots & -k_{sAk_1} & & & & \\ & -k_{sn_1} & k_{sAk_2} & & & & \\ & & & k_{\theta A} & & & \\ -k_{sA1} & & & & k_{eA1}+k_{pA1}+k_{sA1} & -k_{pA1} & \\ & & & & -k_{pA1} & \ddots & -k_{pAk_2} \\ & & & & & -k_{pAk_2} & k_{pAk_2}+k_{eAk_2} \end{bmatrix}$$

$$C_A = \begin{bmatrix} c_{sA1}+c_{sA2} & -c_{sA2} & & & -c_{sA1} & & \\ -c_{sA2} & \ddots & -c_{sAk_1} & & & & \\ & -c_{sAk_1} & c_{sAk_2} & & & & \\ & & & c_{\theta A} & & & \\ -c_{s1} & & & & c_{eA1}+c_{pA1}+c_{sA1} & -c_{pA1} & \\ & & & & -c_{pA1} & \ddots & -c_{pAk_2} \\ & & & & & -c_{pAk_2} & c_{pAk_2}+c_{eAk_2} \end{bmatrix}$$

$$M_{gA} = \begin{bmatrix} m_{sA1} & & & & & & \\ & \ddots & & & & & \\ & & m_{sAk_1} & & & & \\ & & & \sum_{i=1}^{k_1} m_{sAi} h_{sAi} & & & \\ & & & & m_{eA1}+m_{pA1} & & \\ & & & & & \ddots & \\ & & & & & & m_{eAk2}+m_{pAk_2} \end{bmatrix}$$

$$\ddot{X}_{fgA} = \left\{ x_{fgA1}, \ldots, x_{fgAi}, \ldots, x_{fgA(n_1+1)}, \ldots, x_{fgAn} \right\}^T$$

$$\ddot{x}_{fgAi} = \begin{cases} \ddot{x}_g & 1 \le i \le k_1 + 1 \\ \ddot{x}_g - (m_{eAi}\ddot{x}_{fAi} + c_{eAi}\dot{x}_{fAi} + k_{eAi}x_{fAi})/m_{pAi} & k_1 + 1 < i \le n_1 \end{cases}$$

$$n_1 = k_1 + k_2 + 1$$

Similarly, the equations of motion of superstructure, platform rotation and substructure of structure B can be expressed as

$$\begin{aligned} & M_{sB}\ddot{X}_{sB} + C_{sB}\dot{X}_{sB} + K_{sB}X_{sB} \\ & \quad = -M_{sB}I_{B_1}\ddot{x}_g - M_{sB}H_B\ddot{\theta}_B - B_{sB}U \end{aligned} \tag{5}$$

$$\sum_{i=1}^{n_1} m_{sBi}h_{Bi}(\ddot{x}_g + \ddot{x}_{sBi} + h_{Bi}\ddot{\theta}_B) + c_{\theta B}\dot{\theta}_B + k_{\theta B}\theta_B = 0 \tag{6}$$

$$\begin{aligned} & M_{dB}\ddot{X}_{dB} + C_{dB}\dot{X}_{dB} + K_{dB}X_{dB} \\ & \quad = -M_{pB}I_{B_2}\ddot{x}_g + M_{eB}\ddot{X}_{fB} + C_{eB}\dot{X}_{fB} + K_{eB}X_{fB} \end{aligned} \tag{7}$$

where M_{sB}, C_{sB} and K_{sB} are respectively the $J_1 \times J_1$ mass, damping and stiffness matrices of the superstructure. $\ddot{X}_{sB}$, $\dot{X}_{sB}$ and X_{sB} are respectively the J_1-dimensional acceleration, velocity and displacement vectors of the superstructure; M_{dB}, C_{dB} and K_{dB} are respectively the $J_2 \times J_2$ mass, damping and stiffness matrices of the substructure; $\ddot{X}_{dB}$, $\dot{X}_{dB}$ and X_{dB} are respectively the J_2-dimensional acceleration, velocity and displacement vectors of the substructure; M_{eB}, C_{eB} and are respectively the $J_2 \times J_2$ mass, damping and stiffness matrices of the equivalent soil; $\ddot{X}_{fB}$, $\dot{X}_{fB}$ and X_{f2} are respectively the J_2-dimensional acceleration, velocity and displacement vectors of unit soil column; $\ddot{x}_g$ is the ground acceleration; $c_{\theta B}$ and $k_{\theta B}$ are respectively the damping and stiffness coefficients of the platform rotation; θ_B is the rotation angle of the platform; M_{pB} is a $J_2 \times J_2$ mass matrix of the pile group; I_{B_1} and I_{B_2} are the identity vectors, H_B is a J_1-dimensional height vector of the building floors, U is the control force matrix, and B_{sB} is the location matrix of the control forces. Equations (5)to (7) can be written as an equivalent equation:

$$M_B\ddot{X}_B + C_B\dot{X}_B + K_BX_B = -M_{gB}\ddot{X}_{fgB} - B_{sB}U \tag{8}$$

where M_B, C_B and K_B are respectively the $n_2 \times n_2$ mass, damping and stiffness matrices of system B; $\ddot{X}_B$, $\dot{X}_B$ and X_B are respectively the n_2-dimensional acceleration, velocity and displacement vectors of system B; M_{gB} is the diagonal matrix of M_B; $\ddot{X}_{fgB}$ is the acceleration vector of free field input. The matrices can be expressed as follows:

$$M_B = \begin{bmatrix} m_{sB1} & & & m_{sB1}h_{sB1} & & & \\ & \ddots & & \vdots & & & \\ & & m_{sBJ_1} & m_{sBk_1}h_{sBJ_1} & & & \\ m_{sB1}h_{sB1} & \cdots & m_{sBJ_1}h_{sBJ_1} & \sum_{i=1}^{J_1} m_{sBi}h_{sBi} & & & \\ & & & & m_{eB1}+m_{pB1} & & \\ & & & & & \ddots & \\ & & & & & & m_{eBJ2}+m_{pBJ_2} \end{bmatrix}$$

$$K_B = \begin{bmatrix} k_{sB1}+k_{sB2} & -k_{sB2} & & & -k_{sB1} & & \\ -k_{sB2} & \ddots & -k_{sBJ_1} & & & & \\ & -k_{sBJ_1} & k_{sBJ_2} & & & & \\ & & & k_{\theta A} & & & \\ -k_{sB1} & & & & k_{eB1}+k_{pB1}+k_{sB1} & -k_{pB1} & \\ & & & & -k_{pB1} & \ddots & -k_{pBJ_2} \\ & & & & & -k_{pBJ_2} & k_{pBJ_2}+k_{eBJ_2} \end{bmatrix}$$

$$C_B = \begin{bmatrix} c_{sB1}+c_{sB2} & -c_{sB2} & & & -c_{sB1} & & \\ -c_{sB2} & \ddots & -c_{sBJ_1} & & & & \\ & -c_{sBJ_1} & c_{sBJ_2} & & & & \\ & & & c_{\theta B} & & & \\ -c_{sB1} & & & & c_{eB1}+c_{pB1}+c_{sB1} & -c_{pB1} & \\ & & & & -c_{pB1} & \ddots & -c_{pBJ_2} \\ & & & & & -c_{pBJ_2} & c_{pBJ_2}+c_{eBJ_2} \end{bmatrix}$$

$$M_{gB} = \begin{bmatrix} m_{sB1} & & & & & & \\ & \ddots & & & & & \\ & & m_{sBJ_1} & & & & \\ & & & \sum_{i=1}^{J_1} m_{sBi}h_{sBi} & & & \\ & & & & m_{eB1}+m_{pB1} & & \\ & & & & & \ddots & \\ & & & & & & m_{eBJ_2}+m_{pBJ_2} \end{bmatrix}$$

$$\ddot{X}_{fgB} = \left\{x_{fgB1}, \ldots, x_{fgBi}, \ldots, x_{fgB(J_1+1)}, \ldots, x_{fgBn_2}\right\}^T$$

$$\ddot{x}_{fgBi} = \begin{cases} \ddot{x}_g & 1 \le i \le J_1 + 1 \\ \ddot{x}_g - (m_{eBi}\ddot{x}_{fBi} + c_{eBi}\dot{x}_{fBi} + k_{eBi}x_{fBi})/m_{pBi} & J_1 + 1 < i \le n_2 \end{cases}$$

$$n_2 = J_1 + J_2 + 1$$

Equations (4) and (8) can be written as an equivalent equation:

$$M\ddot{X} + C\dot{X} + KX = -M_g\ddot{X}_{fg} + B_sU \tag{9}$$

where

$$M=\begin{bmatrix} M_A & \\ & M_B \end{bmatrix};\quad K=\begin{bmatrix} K_A & \\ & K_B \end{bmatrix};\quad C=\begin{bmatrix} C_A & \\ & C_B \end{bmatrix};$$
$$M_g=\begin{bmatrix} M_{gA} & \\ & M_{gB} \end{bmatrix};\quad B_s=\begin{bmatrix} B_{sA} & B_{sB} \end{bmatrix}^T;$$
$$\ddot{X}_{fg}=\begin{bmatrix} \ddot{X}_{fgA} & \ddot{X}_{fgB} \end{bmatrix}^T$$

$\ddot{X}$, $\dot{X}$ and X are respectively the equivalent acceleration, velocity and displacement vectors of the combined system.

3. Responses of unit soil column

In this paper, a unit soil column is taken as the free field model. Assuming that the free field soil can be divided into S layers from top to bottom, their lumped mass is

$$m_{fi}=\begin{cases} \frac{1}{2}\rho_1 h_1 & i=1 \\ \frac{1}{2}(\rho_{i-1}h_{i-1}+\rho_i h_i) & i>1 \end{cases} \tag{10}$$

where h_i and ρ_i are respectively the height and density of the i-th layer The horizontal stiffness of the i-th layer is

$$k_{fi}=\frac{G_i}{h_i} \tag{11}$$

where G_i is the shear modulus of the i-th layer. The damping matrix of the unit soil column C_f is

$$C_f=M_f\alpha_f+K_f\beta_f \tag{12}$$

where α_f and β_f can be calculated by

$$\alpha_f=\begin{bmatrix} \alpha_1 & & \\ & \ddots & \\ & & \alpha_s \end{bmatrix},\quad \beta_f=\begin{bmatrix} \beta_1 & & \\ & \ddots & \\ & & \beta_s \end{bmatrix},$$
$$\alpha_i=\xi_i\omega_i,\quad \beta_i=\frac{\xi_i}{\omega_i},\quad \omega_i=\frac{\pi}{2h_i}\sqrt{\frac{G_i}{\rho_i}}$$

where $i=1(\ldots)S)$ ξ_i is the damping ratio of the i-th layer. Thus, the dynamic equation of motion of the unit soil column is

$$M_f\ddot{X}_f+C_f\dot{X}_f+K_fX_f=-M_f\ddot{x}_g \tag{13}$$

where the damping ratio of soil is 0.05. The motion equation can be solved with Newmark-β method.

4. Mass, stiffness and damping of equivalent soil column

During the vibration of the pile group, the associated mass includes the mass of the piles and the additional mass of the surrounding soil. The additional mass can be obtained approximately by

$$m_{ei}=\rho A h_i \tag{14}$$

where ρ is the density of the soil, A is the area of platform and h_i is the height of the i-th layer of soil.

Based on the Mindlin method, the horizontal stiffness of the soil can be calculated approximately by (Li and Sun, 2002; Zou et al., 2004)

$$\begin{aligned} k_{ei}(z_i)=&\frac{8\pi E(z_i)}{3}\left\{\sinh^{-1}\frac{L_i-z_i}{r_i}\right\}+\sinh^{-1}\frac{L_i+z_i}{r_i} \\ &+\frac{2}{3r_i^2}\left[\frac{r_i^2L_i-2r_i^2z_i+L_iz_i^2+z_i^3}{(r_i^2+(L_i+z_i)^2)^{0.5}}-\frac{-2r_i^2z_i+z_i^3}{(r_i^2+z_i^2)^{0.5}}\right] \\ &-\frac{2}{3}\left[\frac{z_i-L_i}{(r_i^2+(L_i-z_i)^2)^{0.5}}-\frac{z_i}{(r_i^2+z_i^2)^{0.5}}\right] \\ &\times\frac{4}{3}\left[\frac{r_i^2z_i+L_iz_i^2+z_i^3}{(r_i^2+(L_i+z_i)^2)^{1.5}}+\frac{r_i^2z_i+z_i^3}{(r_i^2+z_i^2)^{1.5}}\right]\Bigg\}^{-1} \end{aligned} \tag{15}$$

where $E(z_i)$ is the Young's Modulus of the soil at depth z_i, and L_i is the length of the i-th pile segment.

The horizontal damping of the soil can be obtained from

$$\begin{cases} c_{e1}=2R_p h_1\rho_1(\mathrm{v}_{p1}+\mathrm{v}_{s1}) \\ c_{ei}=2R_p[h_i\rho_i(\mathrm{v}_{pi}+\mathrm{v}_{si})+h_{i+1}\rho_{i+1}(\mathrm{v}_{p,i+1}+\mathrm{v}_{s,i+1}) \end{cases} \tag{16}$$

where R_p is the pile radius, h_i is the height of the i-th soil layer, v_p is the P wave velocity and v_s is the shear-wave velocity.

$$\mathrm{v}_p=\sqrt{(\lambda+2G)/\rho}$$

$$\lambda=\mu E/[(1+\mu)(1-2\mu)]$$

where μ is Poisson's ratio and G is the shear modulus.

5. Control equation and its solution

In state space, equation (9) becomes

$$\dot{Z}=AZ+BU+E \tag{17}$$

where

$$Z = \begin{bmatrix} X \\ \dot{X} \end{bmatrix},$$

$$A = \begin{bmatrix} \mathbf{0} & \mathbf{0} & I_A & \mathbf{0} \\ \mathbf{0} & \mathbf{0} & \mathbf{0} & I_B \\ -M_A^{-1}K_A & \mathbf{0} & -M_A^{-1}C_A & \mathbf{0} \\ \mathbf{0} & -M_B^{-1}K_B & \mathbf{0} & -M_B^{-1}\mathbf{C}_B \end{bmatrix}$$

$$B = \begin{bmatrix} \mathbf{0} \\ \mathbf{0} \\ M_A^{-1}B_{sA} \\ -M_B^{-1}B_{sB} \end{bmatrix}, \quad E = \begin{bmatrix} \mathbf{0} \\ \mathbf{0} \\ -I_A\ddot{x}_g \\ -I_B\ddot{x}_g \end{bmatrix}$$

The classical LQR method is employed to design the controllers. The index of control performance can be expressed as

$$J = \frac{1}{2}\{Z-\alpha\}^T S\{Z-\alpha\} + \frac{1}{2}\int_0^{t_f} \{Z-\beta\}^T Q\{Z-\beta\} + U^T dt \tag{18}$$

where S, $Q = 2n \times 2n$ weighting matrices of response, $R = n \times n$ weighting matrix of control force, t_f is the time of control end, $\alpha = 2n \times 1$ is the expected steady response vector in t_f and $\beta = n \times 1$ is the expected instantaneous response vector in t_f. Assuming $t_f = \infty$, $\lim_{t_f \to 0} Z = 0$, $\alpha = 0$, and $\beta = 0$, and so equation (18) can be rewritten as

$$J = \frac{1}{2}\int_0^{t_f} Z(t)^T QZ(t) + U^T RU(t)dt \tag{19}$$

Generally, the performance of an optimal closed loop control system is determined by the ratio of Q and R. Increasing Q or reducing R will increase the control force and enhance the gain feedback of the control system, thus decreasing the amplitude of dynamic response. Therefore a reasonable determination of Q and R will be very important for the design of the control system. In this paper, Q and R are determined using

$$Q = \alpha_1 \begin{bmatrix} K & \\ & M \end{bmatrix}, \quad R = \beta_1 I \tag{20}$$

where α_1 and β_1 are the undetermined coefficients related to the constants of the controller, which are used to adjust the values of Q and R. Investigations show that the response and the control force are related only to the ratio of α_1 to β_1. The optimal control forces may be obtained by minimizing the objective function J in equation (19) with the constraints of equation (9). According to the extreme value principle, we have

$$U(t) = -R^{-1}B^T\lambda \tag{21}$$

$$\lambda = PZ(t) \tag{22}$$

$$U(t) = -GZ(t) \tag{23}$$

where

$$G = R^{-1}B^T P \tag{24}$$

G is the optimal state feedback gain matrix; $\lambda = 2n \times 1$ Lagrange operator vector; $P = 2n \times 2n$ Riccati matrix, determined by

$$\dot{P} = PA + A^T P - PBR^{-1}B^T P + Q \tag{25}$$

For a non-time-varying system, P can be considered as a constant matrix. Thus equation (25) can be simplified as

$$PA + A^T P - PBR^{-1}B^T P + Q = 0 \tag{26}$$

To avoid time delay, equation (26) can be solved offline by iteration methods.

6. Numerical simulation

A complex of two adjacent pile-foundation frame structures, structure A and structure B, are considered, as shown in Figure 1. Structure A is a six-story frame structure on a piled foundation. Its mass and stiffness coefficients at each story unit are $m_i = 2.0 \times 10^4$ kg and $k_i = 2 \times 10^5$ kN/m, respectively, and the span and height of each story are 6m and 4m respectively. The dimensions of the foundation platform are 8m × 8m × 1m, supported by four reinforced concrete piles, each 20m long and with cross-section 0.3m × 0.3m, located under each column; Structure B is a 10-story frame structure with a piled foundation. Its mass and stiffness coefficients at each story unit are $m_j = 1.8 \times 10^5$ kg and $k_j = 1.6 \times 10^5$ kN/m, respectively, and the span and the height of each storey are 5m and 4m respectively. The dimensions of the foundation platform are 8m × 8m × 0.8m, supported by four reinforced concrete piles, each 20m long and with cross-section 0.3m × 0.3m, located under each column. The damping ratio of the structures $\xi = 0.05$ (Rayleigh model). The control actuator of the ideal hydraulic servo-system is located at the sixth floor. The 1940 El Centro earthquake (north-south component) scaled to a maximum acceleration of 0.2 g is used as the input excitation, with a duration of 20s. The parameters of each soil layer are shown in Table 1.

Table 1. Parameters of soil layers

F	Thickness/*m*	μ	Density/$g.cm^{-3}$	$v_s/m.s^{-1}$
1	1.0	0.45	1.99	190
2	3.5	0.40	1.82	245
3	2.0	0.45	2.04	206
4	3.8	0.40	1.82	280
5	6.5	0.45	2.06	351
6	10.0	0.40	1.90	350
7	20.0	0.45	2.00	400

To obtain an optimum control effect, the coefficients of the weighting matrices are $\alpha_1 = 100$, $\beta_1 = 8 \times 10^{-8}$ respectively.

6.1. Influence of PSSI on control

On the basis of the above conditions, the time histories of displacement, inter-story drift, top floor acceleration and control force, both including and excluding the PSSI, were obtained as shown in Figures 2–8. It can be seen that the PSSI of the structure has a distinct influence on the effect of control. When the PSSI is considered, the displacement, inter-story drift and top floor acceleration of structure A are much larger than when there is no PSSI. The maximum difference in displacements approaches 12%, and the maximum difference in acceleration approaches 15%. Nevertheless, when the PSSI is considered, the displacement and the top-floor inter-story drift of structure B are a little smaller than those with no PSSI, and the acceleration is a little larger than with no PSSI. The maximum difference in displacement response is about 5%, and the maximum difference in acceleration is about 3%. Generally, the influence of PSSI on structure A is larger than on structure B. The PSSI of structure A enlarges, and that of structure B reduces the seismic responses. There are several reasons for the PSSI influence on structure A: a) The PSSI increases the natural period of the structure making it more flexible. b) Due to the flexible support, the pure horizontal motion of the structure caused by the earthquake input changes to a combination of horizontal and rotational motion. c) When the PSSI is considered, there exists an energy exchange between the structures and the soil, with some of the vibration energy dissipating directly into the soil. At the same time, the control force increases slightly when SSI is considered, depending on the structural and control parameters. When SSI is considered there is a larger displacement response, which requires a larger control force to overcome.

Generally, the influence of PSSI on vibration control for structure A is much larger than that of structure B.

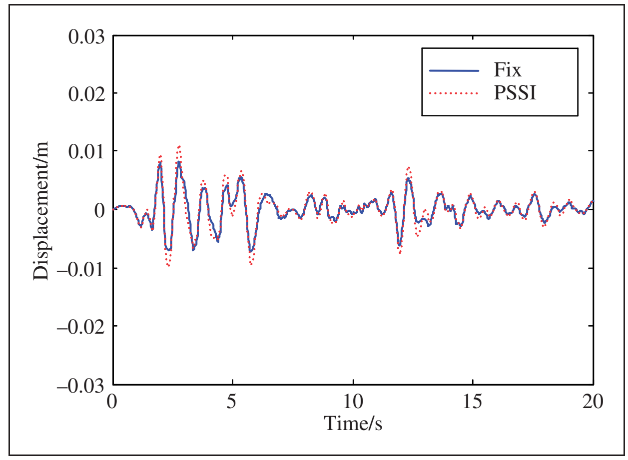

Figure 2. Displacement of top floor of structure A.

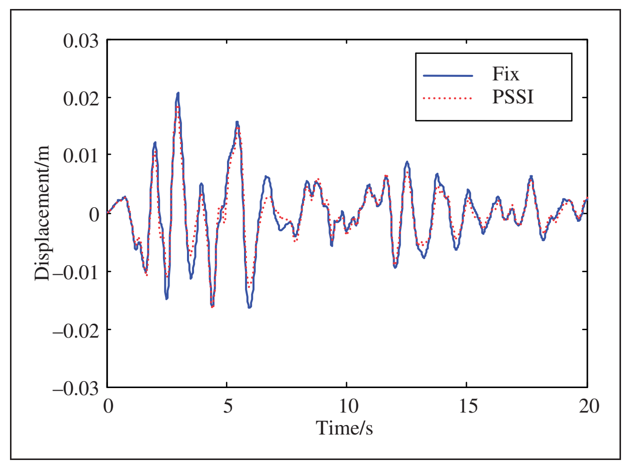

Figure 3. Displacement of top floor of structure B.

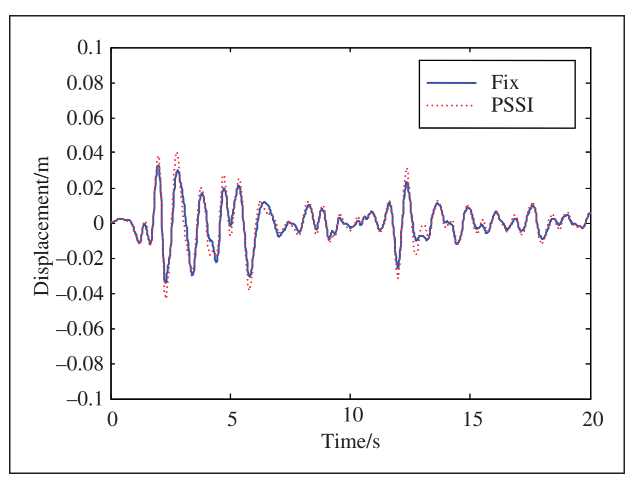

Figure 4. Inter-story drift of top floor of structure A.

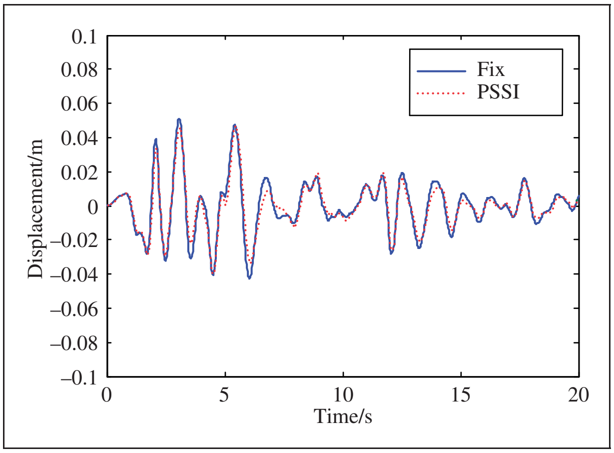

Figure 5. Inter-story drift of top floor of structure B.

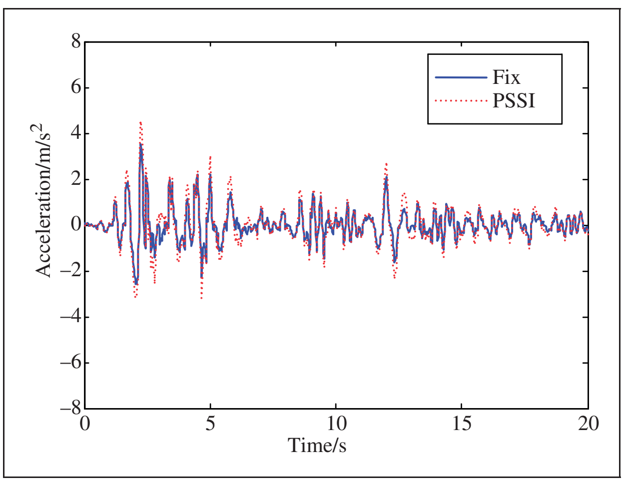

Figure 6. Acceleration of top floor of structure A.

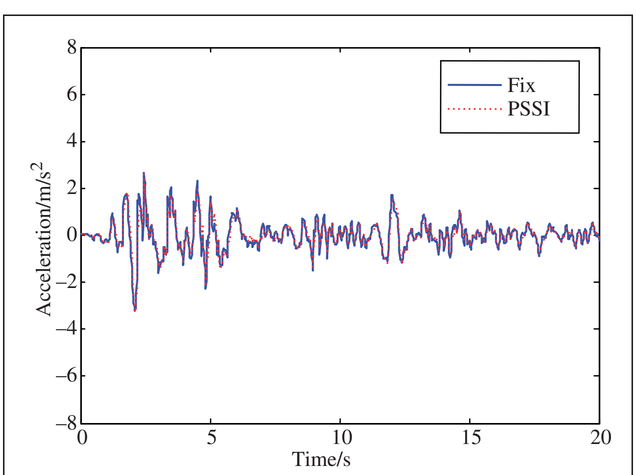

Figure 7. Acceleration of top floor of structure B.

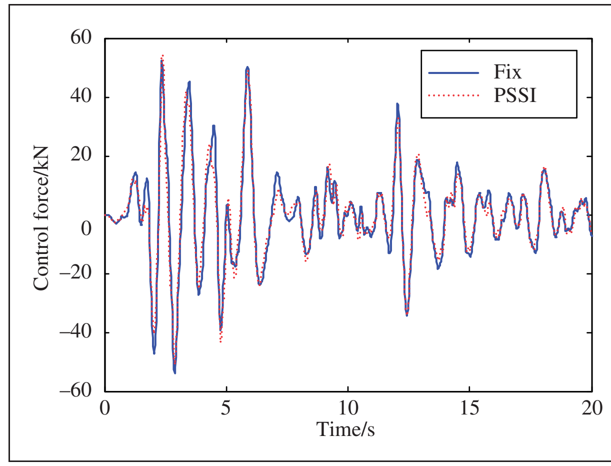

Figure 8. Time history of control force.

The main reason is that the stiffness of structure A is larger than that of structure B. When PSSI is considered, structure B will accept the support from adjacent structure A more readily because of their asynchronous vibration. Thus, when the structural and control parameters are reasonable, the seismic response of structure B will reduce because of PSSI.

However, the change of control force due to PSSI is not very obvious (no more than a 3% increase). The main reason is that, for adjacent buildings, the control force depends mainly on their asynchronous motion. The PSSI of adjacent buildings has obvious influences on their responses, but alteration of their asynchronous motion is not marked. This is useful for the control of adjacent buildings because the PSSI model of adjacent buildings is more difficult to build than that of a single building.

6.2. Influence of shear-wave velocity of soil

Types of construction sites may be classified by the equivalent shear-wave velocity and the thickness of the soil layer. In order to investigate the influence of shear-wave velocity on a controlled structure, assume that other conditions remain unchanged and that the ground is composed of a single soil type. Taking the response to a shear-wave velocity of 100m/s as a standard value, the ratios of responses to standard values, which are named response factors, were obtained and are shown in Figure 9. The figure shows that with increasing shear-wave velocity, the displacements of both structures A and B decrease gradually. The bigger the shear-wave velocity, the more gradual is the trend in the response curves. When the equivalent shear-wave velocity approaches 550m/s, the displacement responses approach constant values. The acceleration response of both structures increases gradually

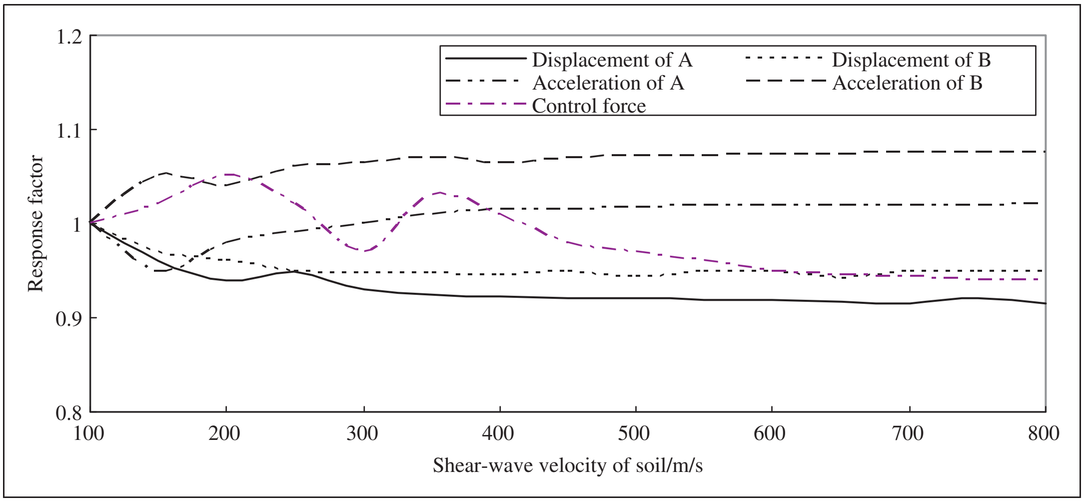

Figure 9. Response factor variation with equivalent shear wave velocity of soil.

with increasing shear-wave velocity, and the rate of increase decreases with increasing shear-wave velocity. When the equivalent shear-wave velocity approaches 450m/s, the acceleration response tends to a constant value. Generally, the range of variation of structure B is much greater than that of structure A, the main reason being that the shear-wave velocity affects the structures by changing their horizontal and rotational stiffnesses. When the shear-wave velocity increases, the horizontal and rotational stiffnesses of structure A become larger, and its displacement response will decrease. However, when the shear-wave velocity reaches a certain value, the constraint stiffness of the soil approaches the stiffness of a fixed foundation. Hence, the change of response of structure A will then become more gradual. In general, the change of response for structure B should have a similar trend to that of structure A. However, it is linked to structure A, and hence its motion will be restrained by structure A.

As for the change in control force, with increasing shear-wave velocity, the control force of the system decreases gradually. The reason is that the increase of shear-wave velocity leads to the reduction of displacement response of the structural system, and thus the energy input required for control decreases accordingly.

6.3. Influence of pile length

Previous research has shown that the influence of substructure stiffness on PSSI cannot be neglected. In order to investigate the influence of pile length on the PSSI of our controlled structures, let other conditions be unchanged and take the response based on 5m long piles as a standard value. The ratios of peak values of response to standard values were obtained and found to vary with changing pile length as shown in Figure 10. It can be seen from this figure that as the pile length increased, the displacement of both structures A and B and also the acceleration of structure B decreased gradually, and the acceleration of the top floor of structure A initially increased before tending to a stationary value when the pile length approached 20m. All responses tended to approach constant values with increasing shear-wave velocity. The main reason for the observed behavior is that the PSSI occurs mainly in the upper layer of soil. When the piles are long enough, the influence of the deeper sections of the piles on the horizontal and rotational structural stiffness, which is mainly caused by the upper layer of soil, is relatively limited. The control force response factor fluctuated about 1 with increasing pile length, with no obvious rule governing its variation, before tending to a constant value of approximately 0.99 for pile lengths over 40m. The initial fluctuations were, however, of small amplitude.

6.4. Influence of pile diameter

In order to investigate the influence of pile diameter on the controlled structures, we hold all other conditions unchanged and take the response based on 0.1m diameter piles as a standard value, with the ratios of calculated responses to standard values, (response factor), obtained and shown in Figure 11. The figure shows that with increasing pile diameter, the displacement of structure A decreases initially, tending to a stationary value for pile diameters exceeding 0.45m. The displacement of structure B decreases similarly to structure A up to a pile diameter of 2.3m before gradually returning to a displacement factor just below 1 at 0.85m pile diameter. Simultaneously the accelerations of structures A and B increase gradually with increasing pile

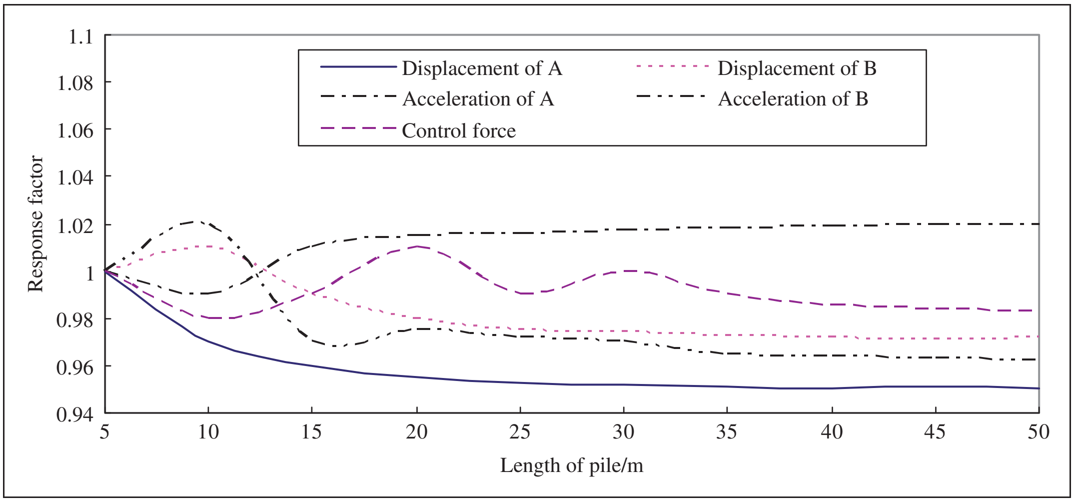

Figure 10. Response factor variation with pile length.

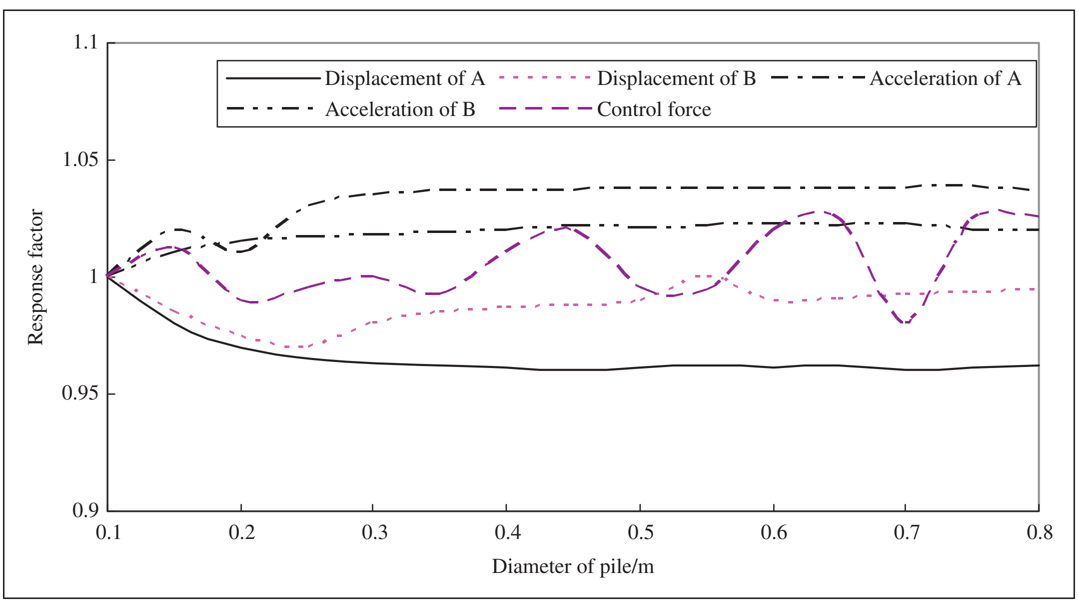

Figure 11. Response factor variation with pile diameter.

diameter before stabilizing at acceleration factors of approximately 1.04 (A) and 1.02 (B) for pile diameters exceeding 0.3m. The reason for the observed behavior is that the PSSI depends on the horizontal and rotational stiffness of the structure base, which in turn depends on the stiffness of the soil and base. When the stiffness of the base approaches a particular value, the soil stiffness becomes the most important parameter affecting PSSI. Consequently, it may be concluded that it is not an economical solution to increase the pile diameter in order to reduce the PSSI of structures. Similar to the variation with pile length, the control force factor oscillated with small amplitude about a mean of approximately 1, but with no obvious governing rule.

7. Conclusions

The PSSI between a pair of adjacent buildings with piled foundations has an obvious influence on the vibration responses observed during the controlled reaction of the adjacent structures (using two inter-building actuators for control) to seismic ground motion. The resulting variation in the control force was small and did not follow any obvious rule. The influences have been shown to be affected not only by the shear-wave velocity of the soil and the length and diameter of the piles but also by the relative stiffness of the adjacent buildings. Generally, the larger the relative stiffness of the buildings the larger is the influences of PSSI on the buildings. Because the PSSI occurs mainly in the upper layer of soil there is little observable effect or benefit from extending piles much below this layer. When the piles are long enough, the influence of the deeper sections of the piles on the horizontal and rotational structural stiffness, which is mainly caused by the upper layer of soil, is relatively limited. It was also observed that the system became insensitive to pile diameter above about 0.3m. The reason for this is that the PSSI depends on the horizontal and rotational stiffness of the structure base, which in turn depends on the stiffness of the soil and base. When the stiffness of the base approaches a particular value, the soil stiffness becomes the most important parameter affecting PSSI. Consequently, it may be concluded that it is not an economical solution to arbitrarily increase the pile diameter in order to reduce the PSSI of structures.

Funding

This work was supported by Fuzhou University (grant number 0460).

References

Basili M and Angelis MD (2007) Optimal passive control of adjacent structures interconnected with nonlinear hysteretic devices. *Journal of Sound and Vibration* 301(1–2): 106–125.

Kobori T, Yamada T and Takenaka Y (1988) Effect of dynamic tuned connector on reduction of seismic response – application to adjacent office buildings. In *Proceedings of the Ninth World Conference Earthquake Engineering*. Vol. 5, Tokyo-Kioto Japan, pp. 773–778.

Li YM and Sun GF (2002) Dynamic interaction of pile-soil-frame structure. *Journal of Building Structure* 23(2): 75–81.

Lin CC, Chang CC and Wang JF (2009) Active control of irregular buildings considering soil–structure interaction effects. *Soil Dynamics and Earthquake Engineering* 29(1): 1–11.

Lu XL, Xu YL and Yang Z (2002) Seismic control of adjacent buildings using fluid dampers: experimental study. *Advances in Building Technology* 3(2): 973–985.

Luco JE and Barros FCPD (1998) Control of the seismic response of a composite tall building modelled by two interconnected shear beams. *Earthquake Engineering and Structural Dynamics* 27(3): 205–223.

Maki T, Maekawa K and Mutsuyoshi H (2006) RC pile-soil interaction analysis using a 3D-finite element method with fibre theory-based beam elements. *Earthquake Engineering & Structural Dynamics* 35(13): 1587–1607.

Ni YQ, Ko JM and Ying ZG (2001) Random seismic response analysis of adjacent buildings coupled with non-linear hysteretic dampers. *Journal of Sound and Vibration* 246(3): 403–417.

Ni YQ, Ko JM and Ying ZG (2004) Non-linear stochastic optimal control for coupled-structures system of multi-degree-of-freedom. *Journal of Sound and Vibration* 274(3–5): 843–861.

Smith HA and Wu WH (1997) Effective optimal structural control of soil-structure interaction systems. *Earthquake Engineering and Structural Dynamics* 26(5): 549–570.

Smith HA, Wu WH and Borja RI (1994) Structural control considering soil-structure interaction effects. *Earthquake Engineering and Structural Dynamics* 23(6): 609–626.

Wang HD and Shang SP (2006) Computational research on vertical dynamic response of single-pile considering pile-soil interaction during passage of Rayleigh waves. *Engineering Mechanics* 26(3): 2197–2201.

Wong HL and Luco JE (1991) Structural control including soil-structure interaction effects. *Journal of Engineering Mechanics ASCE* 117(10): 2237–2250.

Wu WH and Smith HA (1995) Comparison of SSI effects on externally and internally controlled systems. *Smart Materials and Structures* 4(1a): 158–168.

Zhang G, Pan DZ and Chen JX (2006) Analysis of pile-soil interaction by computer simulation. *Experimental Mechanics in Nano and Biotechnology* Pts 1 and 2: 1531–1534.

Zhang WS and Xu YK (2000) Vibration analysis of two buildings linked by Maxwell model-defined fluid dampers. *Journal of Sound and Vibration* 233(5): 775–796.

Zhu H, Wen Y and Iemura H (2001) A study on interaction control for seismic response of parallel structures. *Computers & Structures* 79(2): 231–242.

Zou LH and Zhao RD (2005) Analysis of the random responses to earthquake of the subsoil-base-interaction isolated system. *Journal of Computational Mechanics* 22(5): 72–76.

Zou LH, Zhao RD and Zhao JC (2004) Analysis of the response to earthquake of the pile-soil-isolated structure interaction. *Journal of Geotechnical Engineering* 26(4): 782–786.